

Transient thermo-piezo-elastic responses of a functionally graded piezoelectric plate under thermal shock

Qi-lin Xiong ^{*1,2} and Xin Tian ^{3a}

¹ Department of Mechanics, Huazhong University of Science & Technology, 1037 Luoyu Road, Wuhan 430074, China

² Hubei Key Laboratory of Engineering Structural Analysis and Safety Assessment, 1037 Luoyu Road, Wuhan 430074, China

³ School of Mechanical Engineering, Xi'an Jiaotong University, Xi'an 710049, China

(Received June 18, 2016, Revised February 05, 2017, Accepted July 03, 2017)

Abstract. In this work, transient thermo-piezo-elastic responses of an infinite functionally graded piezoelectric (FGPE) plate whose upper surface suffers time-dependent thermal shock are investigated in the context of different thermo-piezo-elastic theories. The thermal and mechanical properties of functionally graded piezoelectric plate under consideration are expressed as power functions of plate thickness variable. The solution of problem is obtained by solving the corresponding finite element governing equations in time domain directly. Transient thermo-piezo-elastic responses of the FGPE plate, including temperature, stress, displacement, electric intensity and electric potential are presented graphically and analyzed carefully to show multi-field coupling behaviors between them. In addition, the effects of functionally graded parameters on transient thermo-piezo-elastic responses are also investigated to provide a theoretical basis for the application of the FGPE materials.

Keywords: transient thermo-piezo-elastic responses; thermal shock; multi-field coupling behavior; functionally graded piezoelectric plate

1. Introduction

Due to the direct and converse piezoelectric effect, piezoelectric ceramics and composites have been extensively used in many engineering applications such as sensors, actuators, intelligent structures, etc. (Muralt 2008, Starr and Wang 2015, Lin *et al.* 2016, Bidgoli *et al.* 2015, Mohammadimehr *et al.* 2016). In order to realize multi function of piezoelectric structure, such as thermoelectric induction and elastoelectric effect, it is crucial to acquire a thorough knowledge of the thermo-piezoelectric problem of piezoelectric media.

The thermo-piezoelectric theory was first proposed by Mindlin (1961, 1974) and the corresponding governing equations have been established. However, thermal signal propagates at the infinite speed in Mindlin's theory and this phenomenon is not consistent with physical laws in nature (Shen and Tian 2014). Subsequently, based on the first and the second thermodynamics laws, Chandrasekharaiah (1988) further developed the thermo-piezo-electric theory by generalizing Mindlin's model to account for the finite speed of propagation of thermal disturbances. Tianhu *et al.* (2002) studied the thermo-elastic-piezoelectric effect in two-dimensional generalized thermal shock problem using a hybrid Laplace transformation-finite element method based on G-L theory and investigated the problem of a finite thermo-piezo-electric bar with a moving heat source using

the L-S theory (Tianhu *et al.* 2003, 2007). Babaei and Chen (2008) investigated the dynamic response in a one-dimensional rod subjected to a moving heat source. Recently, Ma and He (2016) studied the dynamic response of a thermo-piezo-elastic rod made of piezoelectric ceramics (PZT-4) subjected to a moving heat source in the context of the fractional order theory of thermoelasticity.

It is well known that due to the complexity (multi-field coupling) associated with the governing expressions of thermo-piezo-elastic problem, the inverse Laplace and Fourier transformation techniques are adopted to solve the governing equations. However, the truncation error introduced in the numerical inversion of transforms (Laplace and Fourier transformation) causes the loss of calculation precision, and the results are not as accurate as by the analytical solutions, so the temperature front does not evolve during the computation, implying that the wave effect of heat conduction cannot be captured correctly (Tian and Shen 2005, Tian *et al.* 2006, 2007). Tian *et al.* (2007) solved the generalized thermo-piezo-elastic problems directly in the time domain by using finite element method. And the finite speed of heat propagation is thus depicted perfectly. Hence, the finite element method is used in the present study for solution of the problem.

Functionally Graded Materials (FGMs), differing from the conventional composite materials whose properties vary abruptly across interfaces between two successive layers, the volume fractions of the FGM constituents vary gradually from one surface to the other. These kinds of materials give a non-uniform microstructure with continuously graded macro-properties. Mechanical responses in FGM structures subjected to external loads can be

*Corresponding author, Ph.D.,
E-mail: xiongql@hust.edu.cn

^a Student

optimized by selecting an appropriate material distribution.

In the past decade, thermomechanical analysis of FGMs has been studied by researchers. Mallik and Kanoria (2007) studied one dimensional thermoelastic disturbance in an infinite isotropic functionally graded medium in the context of generalized thermoelasticity without energy dissipation. Xiong and Tian (2012) investigated two-dimensional thermoelastic behavior in an infinite functionally graded body with a cylindrical cavity using Green-Naghdi model. Recently, Heydarpour and Aghdam (2016) investigated the transient thermoelastic behavior of rotating functionally graded (FG) truncated conical shells subjected to thermal shock with different boundary conditions based on Lord-Shulman (L-S) generalized thermoelastic theory. However, the study on the thermoelastic analysis of functionally graded piezoelectric (FGPE) materials is rarely reported, especially on two dimensional problem of FGPE material.

In the present work, transient thermo-piezo-electric responses of a FGPE plate whose upper surface suffers a zonal time-dependent thermal shock are investigated in the context of different theories of thermo-piezo-elasticity. The thermal and mechanical properties of FGPE plate under consideration are assumed to vary as the power of the plate thickness variable. The problem is solved by solving the finite element governing equations in time domain directly. The results, including temperature, stress, displacement and electric potential are depicted graphically. Comparisons are made in the results obtained by different thermo-piezo-elastic theories. Finally, the effects of functionally graded parameters on the responses are very pronounced.

2. Formulation of problem and basic equations

Let us consider a FGPE plate ($L \geq z \geq 0$, L is the thickness of the plate.) irradiated by a zonal thermal shock polarized along the thickness direction (z -axis). The FGPE plate is graded in the thickness direction (z -axis). A coordinate system (x, y, z) is used for this plane problem. In the present study the electron-hole pairs generation in the FGPE plate induced by thermal shock is neglected.

For a linear, homogeneous, FGPE plate, the generalized field equations can be presented in a unified form as following, and the typical linear constitutive equations of a piezoelectric material under G-L (L-S or C-T) thermo-elasticity (Lord and Shulman 1967, Green and Lindsay 1972) are

$$\sigma_{ij} = C_{ijkl} \varepsilon_{kl} - e_{ijk} E_k - a_{ij} (\theta + \tau_1 \dot{\theta}) \quad (1)$$

$$\rho \eta = a_{ij} \varepsilon_{ij} + d_i E_i + \frac{\rho c_E}{T_0} (\theta + \tau_2 \dot{\theta}) \quad (2)$$

$$D_i = e_{ijk} \varepsilon_{jk} + p_{ij} E_j + d_i (\theta + \tau_1 \dot{\theta}) \quad (3)$$

$$q_i + \tau \dot{q}_i = -k_{ij} \theta_{,j} \quad (4)$$

where a_{ij} is thermal modulus and it shows the coupling strength between thermal field and stress field, e_{ijk} is

piezoelectric coefficients and it shows the coupling strength between electric field and stress field, d_i is pyroelectric constants and it shows the coupling strength between thermal field and electric field.

Setting $\tau = \tau_1 = \tau_2 = 0$, we get field equations for the classical coupled theory of thermo-piezo-elasticity (C-T thermo-piezo-elasticity), whereas when $\tau > 0$ and $\tau_1 = \tau_2 = 0$ the equations reduce to the Lord and Shulman model (L-S thermo-piezo-elasticity) and when $\tau = 0$ but when τ_1 and τ_2 are nonvanishing the equations reduce to the Green and Lindsay model (G-L thermo-piezo-elasticity).

Neglecting body force, free charge, and internal heat generation, the equilibrium equations of thermo-piezo-elastic problem are expressed as

$$\sigma_{ji,j} = \rho \ddot{u}_i \quad (5)$$

$$q_{i,i} + \rho T_0 \dot{\eta} = 0 \quad (6)$$

$$D_{i,i} = 0 \quad (7)$$

The relations between strain ε and displacement (u) and between the electric intensity (E) and electric potential ϕ can be expressed as

$$\varepsilon_{ij} = \frac{1}{2} (u_{i,j} + u_{j,i}) \quad (8)$$

$$E_i = -\phi_{,i} \quad (9)$$

If the FGPE plate is infinite in y -direction, the problem can be considered as a plane strain problem. The components of the displacement are defined by

$$u = u(x, z, t), \quad v = 0, \quad w = w(x, z, t) \quad (10)$$

The constitutive equations for a two dimensional plane problem are expressed as follows

$$\sigma_{xx} = c_{11} u_{,x} + c_{13} w_{,z} + e_{31} \phi_{,z} - a_{11} (\theta + \tau_1 \dot{\theta}) \quad (11)$$

$$\sigma_{zz} = c_{13} u_{,x} + c_{33} w_{,z} + e_{33} \phi_{,z} - a_{33} (\theta + \tau_1 \dot{\theta}) \quad (12)$$

$$\sigma_{xz} = c_{44} (u_{,z} + w_{,x}) + e_{15} \phi_{,x} \quad (13)$$

$$D_x = e_{15} (u_{,z} + w_{,x}) - p_{11} \phi_{,x} \quad (14)$$

$$D_z = e_{31} u_{,z} + e_{33} w_{,x} - p_{33} \phi_{,z} + d_z (\theta + \tau_1 \dot{\theta}) \quad (15)$$

For functionally graded solid we will consider, material properties of a thermoelastic body have the following forms

$$\chi = \chi_0 f(z) \quad (16)$$

where χ denotes symbolic material properties, χ_0 is value of material properties at a defined location and $f(z)$ describes

functionality along thickness direction. In the case of coordinate-independent properties, $f(z) = 1$. We will consider that the function of coordinate $f(z) = (1+z)^n$ in the reference (Khoshgoftar *et al.* 2009), wherein n is called the functionally graded parameter.

For numerical convenience, the following dimensionless quantities are introduced

$$\begin{aligned} x_i^* &= c' \zeta x_i, \quad u_i^* = c' \zeta u_i, \\ t^* (\tau^*, \tau_0^*, \tau_1^*) &= c'^2 \zeta^2 t (\tau, \tau_0, \tau_1) \end{aligned} \quad (17)$$

$$\begin{aligned} \theta^* &= \frac{T - T_0}{T_0}, \quad \sigma^* = \frac{2\sigma}{(c_{33}^0 - c_{13}^0)}, \\ D_i^* &= \frac{2D}{(c_{33}^0 - c_{13}^0) \delta_1}, \quad \phi^* = c' \zeta \delta_1 \phi \end{aligned} \quad (18)$$

where $c'^2 = \frac{c_{33}^0}{\rho^0}$, $\zeta = \frac{\rho^0 c_E^0}{k_{11}^0}$. Without causing ambiguity,

the asterisk symbol of the non-dimensional variables is dropped off in the following for the sake of brevity. In the above equations, a comma followed by a suffix denotes material derivative and a superposed dot denotes the derivative with respect to time.

From the preceding description and the problem we will consider, the initial and boundary conditions may be expressed as:

Initial conditions ($t = 0$)

$$u(x, z, t) = w(x, z, t) = \dot{u}(x, z, t) = \dot{w}(x, z, t) = 0 \quad (19)$$

$$\theta(x, z, t) = \dot{\theta}(x, z, t) = 0, \quad \phi_i = \dot{\phi}_i = 0 \quad (20)$$

Boundary conditions

At $z = 0$,

$$\theta(x, z, t) = \theta_0 H(t) H(x_0 - |x|), \quad \sigma_{zz} = \sigma_{xz} = 0 \quad (21)$$

At $x = 0$,

$$u_x(x, z, t) = 0, \quad \frac{\partial \theta}{\partial x} = 0 \quad (22)$$

At $z \rightarrow L$,

$$u = w = \theta = \phi = 0 \quad (23)$$

Where θ_0 is a given temperature, $H(*)$ is the Heaviside function.

3. Finite element equations

For finite element method, in discrete system the displacement, temperature and the electric potential of any point by amount of element node $\{u^{(e)}\}$, $\{\theta^{(e)}\}$, $\{\phi^{(e)}\}$ can be expressed as

$$\{u\} = [N]_{d \times n} \{u^{(e)}\}, \quad \theta = [N']_n \{\theta^{(e)}\}, \quad \phi = [N']_n \{\phi^{(e)}\} \quad (24)$$

where d represents dimension of the problem studied, n is nodes number of element, and shape functions of displacement, temperature and the electric potential, respectively, are $[N]$, $[N']$, $[N']$. Because the electric potential and temperature are scalar, their shape functions are the same.

Elastic strain, temperature gradient, electric intensity can be expressed as

$$\{\varepsilon\} = [B] \{u^{(e)}\}, \quad \{\theta'\} = [B'] \{\theta^{(e)}\}, \quad \{E\} = [B'] \{\phi^{(e)}\} \quad (25)$$

where $[B]$, $[B']$, $[B']$, respectively, are strain matrix, temperature gradient matrix and the gradient matrix of the electric potential.

According to the equilibrium field equations of thermo-piezo-elastic problem, using generalized variational principle, we obtain at any time

$$\begin{aligned} & \int_V \left[\delta \{\varepsilon\}^T \{\sigma\} + \delta \{\theta'\}^T (q + \tau \dot{q}) - \right. \\ & \left. \delta \{E\}^T \{D\} - \delta \theta \rho T_0 (\dot{\eta} + \tau \ddot{\eta}) \right] dV \\ & = \int_V \delta \{u\}^T (-\rho \{\ddot{u}\}) dV + \int_{A_\tau} \delta \{u\}^T \{T'\} dA \\ & + \int_{A_q} \delta \theta \bar{q} dA + \int_{A_\phi} \delta \phi \bar{h} dA \end{aligned} \quad (26)$$

At the right side of above equation, and T , \bar{q} , \bar{h} respectively, external force vector, external heat flux and the charge density.

The above types and the expressions of elastic strain, temperature gradient, the gradient of the electric potential are substituted into the generalized variational principle, then we get

$$\left\{ \begin{aligned} & \left(\begin{matrix} M_{11}^{(e)} & 0 & 0 \\ 0 & 0 & 0 \\ M_{31}^{(e)} & 0 & M_{33}^{(e)} \end{matrix} \right) \begin{pmatrix} \{\ddot{u}^{(e)}\} \\ \{\ddot{\phi}^{(e)}\} \\ \{\ddot{\theta}^{(e)}\} \end{pmatrix} + \\ & \sum_{e=1}^{ne} \left(\begin{matrix} 0 & 0 & C_{13}^{(e)} \\ 0 & 0 & C_{23}^{(e)} \\ C_{31}^{(e)} & C_{32}^{(e)} & C_{33}^{(e)} \end{matrix} \right) \begin{pmatrix} \{\dot{u}^{(e)}\} \\ \{\dot{\phi}^{(e)}\} \\ \{\dot{\theta}^{(e)}\} \end{pmatrix} \\ & + \left(\begin{matrix} K_{11}^{(e)} & K_{21}^{(e)} & -K_{31}^{(e)} \\ K_{21}^{(e)} & K_{22}^{(e)} & K_{31}^{(e)} \\ 0 & 0 & K_{33}^{(e)} \end{matrix} \right) \begin{pmatrix} \{u^{(e)}\} \\ \{\phi^{(e)}\} \\ \{\theta^{(e)}\} \end{pmatrix} = \begin{pmatrix} F^{(e)} \\ H^{(e)} \\ -Q^{(e)} \end{pmatrix} \end{aligned} \right\} \quad (27)$$

where ne is the number of the element.

$$\begin{aligned} [M_{11}^{(e)}] &= \rho \int_{V^{(e)}} [N]_{d \times n}^T [N]_{d \times n} dV, \\ [M_{22}^{(e)}] &= \rho \chi \int_{V^{(e)}} [N']_n^T [N']_n dV, \end{aligned}$$

$$\begin{aligned}
[M_{31}^{(e)}] &= \int_{V^{(e)}} [N']_n [a][B] dV \\
[M_{32}^{(e)}] &= \int_{V^{(e)}} [N']_n [d][N']_n dV \\
[M_{33}^{(e)}] &= \frac{\rho c_E}{T_0} \int_{V^{(e)}} [N']_n [N']_n dV \\
[C_{31}^{(e)}] &= \int_{V^{(e)}} [N']_n [a][B] dV \\
[C_{32}^{(e)}] &= \int_{V^{(e)}} [N']_n [d][N']_n dV \\
[C_{33}^{(e)}] &= (\rho c_E / T_0) \int_{V^{(e)}} [N']_n [N']_n dV \\
[K_{11}^{(e)}] &= \int_{V^{(e)}} [B]^T [C][B] dV \\
[K_{12}^{(e)}] &= \int_{V^{(e)}} [B]^T [e][N']_n dV \\
[K_{13}^{(e)}] &= \int_{V^{(e)}} [B]^T [a][N']_n dV \\
[K_{22}^{(e)}] &= \int_{V^{(e)}} [B']^T [\rho][B'] dV \\
[K_{33}^{(e)}] &= \int_{V^{(e)}} [B']^T [k][B'] dV \\
F^{(e)} &= \int_{A^{(e)}} [N]_n^T \{T'\} dA \\
H^{(e)} &= \int_{A^{(e)}} [N']_n \bar{h} dA \\
Q^{(e)} &= \int_{A^{(e)}} [N']_n \bar{q} dA
\end{aligned}$$

It is known that the above finite element governing equations is similar to the governing equations of vibration, and therefore this kind of generalized thermo-piezo-elastic problems by solving the finite element governing Eq. (27) can be solved. Finally associating with the initial conditions and boundary conditions, we can solve the finite element governing Eq. (27) in time domain directly. It is worth noting that that convergence of the approximate solution to the exact one can in principle be achieved by increasing the number of the element (ne, "h-FEM") (Schwab 1998).

To validate the numerical model proposed in the present study, the example of Aouadi (2006) was simulated by finite element method. Figs. 1 and 2 compare the numerically predicted temperature and displacement in a semi-space

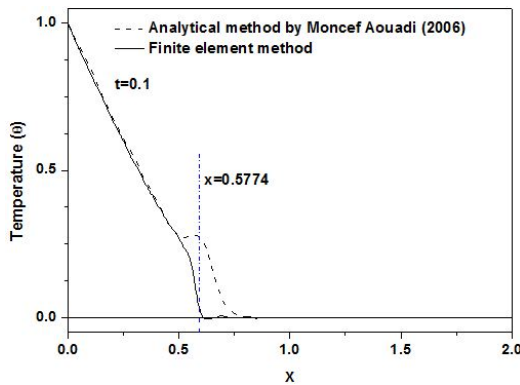


Fig. 1 Comparison of temperature θ predicted with analytical result versus x at $t = 0.1$

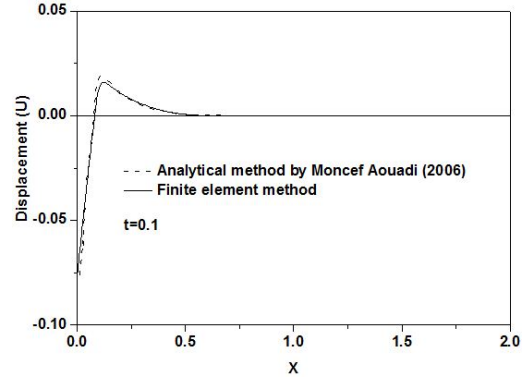


Fig. 2 Comparison of displacement predicted with analytical result versus x at $t = 0.1$

homogeneous piezoelectric medium with those obtained by analytical method (Aouadi 2006). Except for the wave front of the temperature, the agreement between model predictions and analytical results is good, demonstrating the effectiveness of the present numerical model. According to the material parameters (Aouadi 2006), the non-dimensional speed of propagation of thermal wave (temperature) is about $5.7735(1/\sqrt{\tau_0})$, the predictions in the present study are very good (shown in Fig. 1). These results mean the proposed numerical model is reliable.

4. Numerical results and discussion

With the view of illustrating the finite element method presented in the Section 2 in the context of L-S (G-L or C-T) theories of thermo-piezo-elasticity, we now present some numerical results. Cadmium selenide plate was chosen as the material for the purposes of numerical computation, the physical data for which are the following

$$\begin{aligned}
c_{11}^0 &= 74.1Gpa, & c_{13}^0 &= 45.2Gpa, & c_{33}^0 &= 83.6Gpa, \\
c_{44}^0 &= 13.2Gpa, & \rho^0 &= 7600kg/m^3, & c_E^0 &= 420Jkg^{-1}K^{-1}, \\
e_{13}^0 &= -0.160Cm^{-2}, & e_{14}^0 &= -0.138Cm^{-2}, & e_{33}^0 &= 0.347Cm^{-2}, \\
p_{11}^0 &= 8.26 \times 10^{-11}C^2N^{-1}m^{-2}, & p_{22}^0 &= 9.03 \times 10^{-11}C^2N^{-1}m^{-2}, \\
\delta_1 &= -3.92 \times 10^{-12}CN^{-1}, & d_1^0 &= d_z = -2.94 \times 10^{-6}CK^{-1}m^{-2}, \\
a_{11}^0 &= 0.621 \times 10^6NK^{-1}m^{-2}, & a_{22}^0 &= 0.551 \times 10^6NK^{-1}m^{-2}, \\
k_{11}^0 &= k_{33}^0 = 38Wm^{-1}K^{-1}
\end{aligned}$$

The value of thermal relaxation time τ (τ_0, τ_1) for various materials is of the order of seconds (porous materials) to picoseconds (metals) (Vedavarz *et al.* 1994), for metals, the value of thermal relaxation time τ (τ_0, τ_1) ranges from 10^{-14} to 10^{-11} s at room temperature and it is smaller than 10^{-14} s at high temperatures. In the present simulation the thermal relaxation time takes τ (τ_0, τ_1) = 4.695×10^{-14} s. The analytical model is selected as shown in Fig. 3 and the sizes of the model (in which there are OD = 3.0, OB = 3.5) are taken depend on the speed of propagation of thermal wave and elastic wave to ensure that the waves cannot spread to the border during computing time.

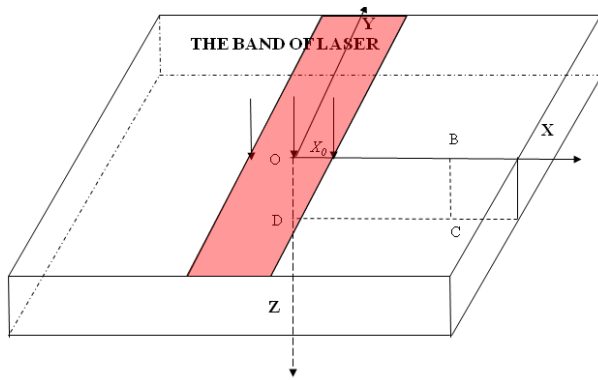


Fig. 3 Three-dimensional model

4.1 Thermo-piezo-elastic responses of homogeneous piezoelectric plate and analysis of thermo-piezo-elastic coupling

Fig. 4 presents the temperature contour of the OBCD region in the context of G-L theory at time instant $t = 0.15$. The purple region represents “zero” temperature variation and the thermal disturbance is restricted in a finite area. As thermal shock is applied along the Z direction (thermal boundary condition), it is clearly observed that the temperature gradient at the wave front along the z direction is much larger than that along the x direction. The sudden jump of the temperature distribution in the position of the heat wave front along z direction (thickness) is shown in Fig. 5.

Fig. 5 shows the distribution of temperature under different thermoelastic theories at time instants, $t = 0.1$ and 0.2 . From Fig. 5, temperature predicted by generalized thermo-piezo-electric theories (L-S and G-L) appears a distinct jump at thermal wave front. At time instant $t = 0.1$, the position of temperature step is about 0.47 and the position becomes 0.92 for time instant $t = 0.2$. The non-dimensional speed of propagation of temperature wave is estimated to be 0.47, which is equal to the value $(1/\sqrt{\tau})$ of theoretical estimation. However, the classical thermo-piezo-electric theory (C-T) cannot describe the finite speed of propagation of thermal wave as shown in Fig. 5.

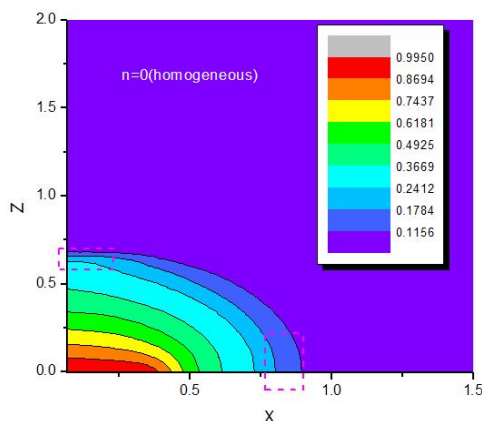


Fig. 4 Temperature contour of rectangle OBCD in the context of thermo-piezo-elastic G-L theory at time instant $t = 0.15$

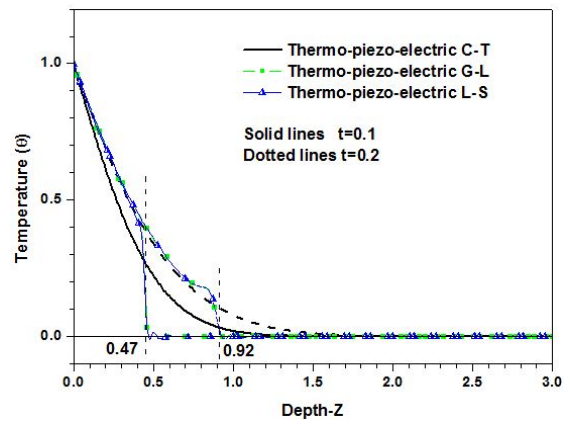


Fig. 5 Temperature θ distribution along edge OD under different thermo-piezo-elastic theories at different time instants

Temperature predicted by the classical thermo-piezo-electric theory significantly differs from that obtained by generalized thermo-piezo-electric theories. Thus, under some extreme load conditions, such as rapid heating, laser shock etc., it is very necessary to use the generalized thermoelastic theory rather than the classical thermoelastic theory for achieving accurate thermal responses in structures.

The distribution of displacement U_z under different thermoelastic theories at time instants, $t = 0.15$ and 0.5 is present at Fig. 6. When the surface of FGPE plate is irradiated by thermal shock, the region near surface of the plate expands to two sides. Outward expansion perpendicular to the surface (X-Y plane) results in the negative displacement and inward expansion causes the positive displacement as shown in Fig. 6. As the time goes on, temperature and thermal expansion increase gradually. Thus, the magnitude of displacement at time instant $t = 0.5$ is larger than that at time instant $t = 0.15$.

When thermal shock is applied to the surface of FGPE plate, thermal expansion occurs suddenly and elastic wave is induced at this moment. The non-dimensional speed of propagation of elastic wave in the FGPE plate is estimated

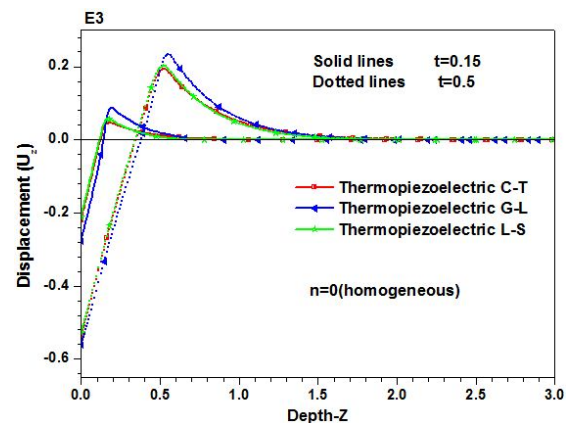


Fig. 6 Displacement U_z distribution along edge OD under different thermo-piezo-elastic theories at different time instants

to be 1.0 by Eq. (5) in Section 2, the location of the elastic wave should be $z = 0.15$ at $t = 0.15$. From Fig. 7, the first peak in stress σ_{zz} curve is caused by elastic wave. Additionally, according to the constitutive relation (Eq. (1)) between stress and strain, $\sigma \approx -a(\theta + \tau_1 \dot{\theta})$, for thermo-piezo-elastic L-S theory ($t_1 = 0$), temperature at the thermal wave front should be linear with stress. From the comparison of Figs. 5 and 7, the prediction of thermo-piezo-elastic L-S theory is correct. For thermo-piezo-elastic G-L theory ($t_1 \neq 0$), although temperature at the thermal wave front is not linear with stress, the position of second peak at stress σ_{zz} curve is corresponding to thermal wave front. For thermo-piezo-elastic C-T theory ($t_1 = 0$), temperature at the thermal wave front is linear with stress as shown in Figs. 5 and 7.

It is worth noting that there are two peaks in the distribution of electric intensity E_z in Fig. 8. According to the constitutive relation of electric intensity, deformation and temperature, $E \approx [-e\varepsilon - d(\theta + \tau_1 \dot{\theta})] / p$, and its curve distribution profile should be corresponding to profiles of strain and temperature distribution, such that the first peak in the distribution of electric intensity E_z is caused by deformation (elastic wave), while the second peak is caused

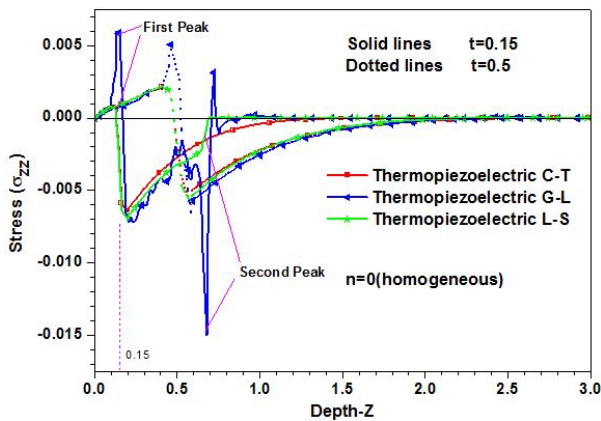


Fig. 7 Stress σ_{zz} distribution along edge OD under different thermo-piezo-elastic theories at time instants $t = 0.15$ and 0.5

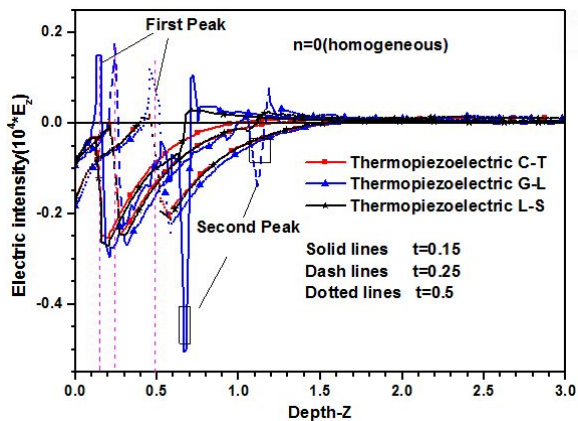


Fig. 8 Electric intensity distribution along edge OD under different thermo-piezo-elastic theories at time instants $t=0.15, 0.25$ and 0.5

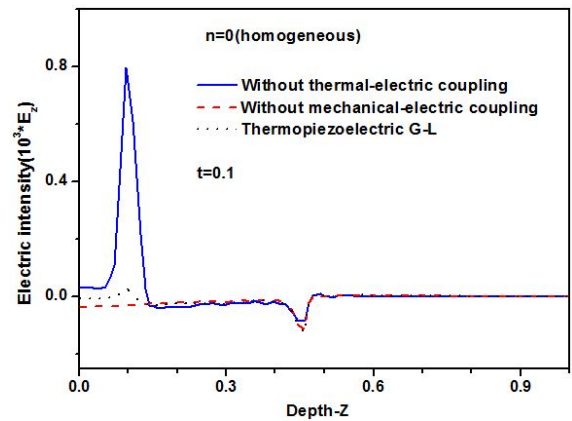


Fig. 9 Comparison of electric intensity between multi-field coupling and non-coupling at time instant $t = 0.1$

by thermal wave. This shows multi-field coupling behavior between thermal field, mechanical field, and electric field. In order to further show the multi-field coupling behavior, the comparison between coupling and non-coupling is shown in Fig. 9 (For non-coupling cases, the corresponding coupling parameters takes zero).

From Fig. 9, it can further show that elastic deformation results in the first peak of electric intensity curve. The first peak in electric intensity curve of the case without thermal-electric coupling is higher than that of thermo-piezo-elastic G-L theory and this phenomenon is understandable. From the constitutive relation $E \approx [-e\varepsilon - d(\theta + \tau_1 \dot{\theta})] / p$, when thermal-electric coupling is included, electric intensity decreases due to the fact that the term of $d(\theta + \tau_1 \dot{\theta})$ is always positive.

4.2 Thermo-piezo-elastic responses of functionally graded piezoelectric plate

To demonstrate the figures clearly, only the numerical results obtained from thermo-piezo-elastic G-L theory are presented in the following figures.

Figs. 10-17 show the distributions of non-dimensional

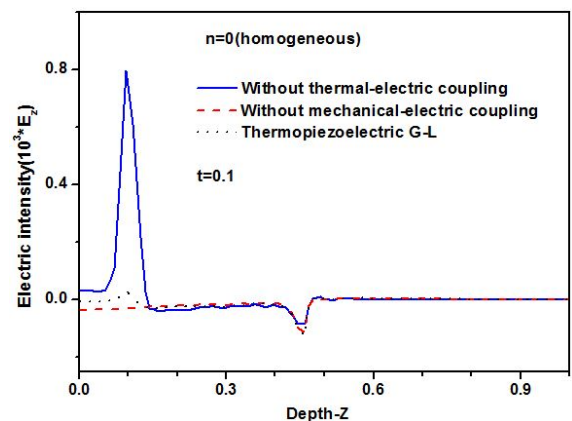


Fig. 10 Temperature θ distribution along edge OD under different functionally graded parameters at time instants $t = 0.15$ and 0.5

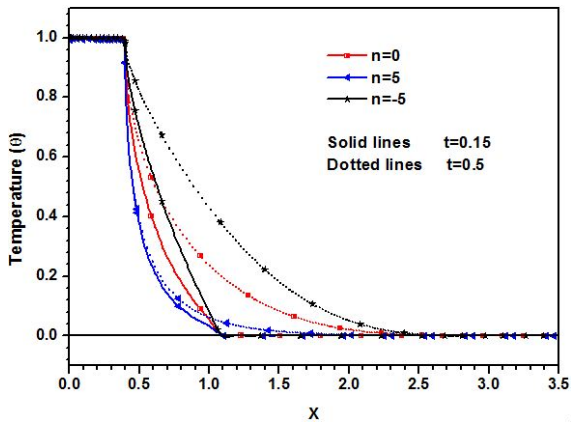


Fig. 11 Temperature θ distribution along edge OB under different functionally graded parameters at time instants $t = 0.15$ and 0.5

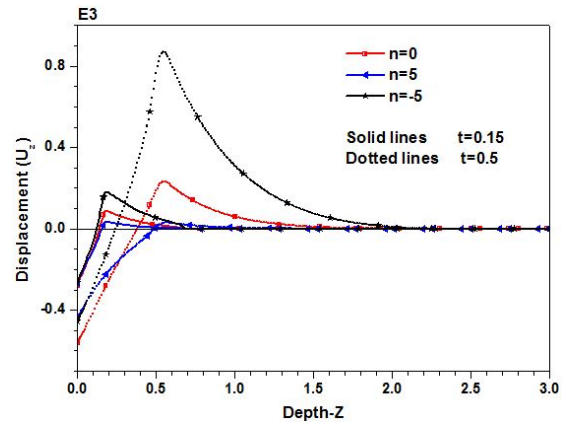


Fig. 12 Displacement U_z distribution along edge OD under different functionally graded parameters at time instants $t = 0.15$ and 0.5

displacement, temperature, stresses and electric potential in the context of thermo-piezo-electric G-L theory at two time instants, namely, $t = 0.15$ and 0.5 .

From Figs. 10-11, it can be seen distinctly that the functionally graded parameter has no any influence on the speed of thermal wave in material but has a significant influence on temperature distribution. The temperature in FGPE of $n = 5$ is lower than in homogeneous case ($n = 0$) for the same location and the temperature in FGPE of $n = -5$ is the highest. Additionally, due to $f(z) = (1+z)^n$ It can be inferred that the effect of functionally graded parameter will increase with the increase of the z coordinate. It should be noted that there is a hump in the thermal wave front for the functionally graded parameter $n = -5$, and the possible reason is that energy cannot be dissipated for $n = -5$.

Figs. 12-13 represent the displacement U_z along edge OD and the displacement U_x along edge OB respectively. It shows a maximum negative value of U_z at the upper surface of the plate and then starts to increase with the increase of thickness distance z and then decreases finally to diminish. And there is a maximum value of U_x at the edge of thermal shock zone and then starts to decrease with the increase of the distance x and then finally diminishes. The reason of

this phenomenon is the expansion parallel to the surface (X-Y plane) leads to the displacement along X direction. Due to the fact that both load distribution and numerical model are symmetry on the Z-Y plane, the displacement U_x at the position of $X = 0$ should be zero. With the increase of the distance from $X = 0$, the displacement U_x increases gradually, which is understandable. In fact, the displacement U_x is the deformation Δ , $\Delta = \epsilon_T L$, here e_T is the thermal strain, L is the distance between the present position and $X = 0$. Thus, at the region near edge of heating area, the displacement U_x reaches the maximum value. Over the heated area, the displacement U_x decreases gradually with the decrease of thermal strain.

For the functionally graded parameter $n = 5$, the displacement is smaller than in homogeneous material ($n = 0$) and the displacement in material of $n = -5$ is larger.

Figs. 14-15 show the distribution of stress σ_{zz} along edge OD and stress σ_{xx} along edge OB respectively. From Fig. 14, the first peak in stress σ_{zz} curve is caused by elastic wave according to the previous discussion. It shows that when the functionally graded parameter $n = 5$, the stress σ_{zz} is greater with respect to the homogeneous material ($n = 0$), and when the functionally graded parameter $n = -5$, the

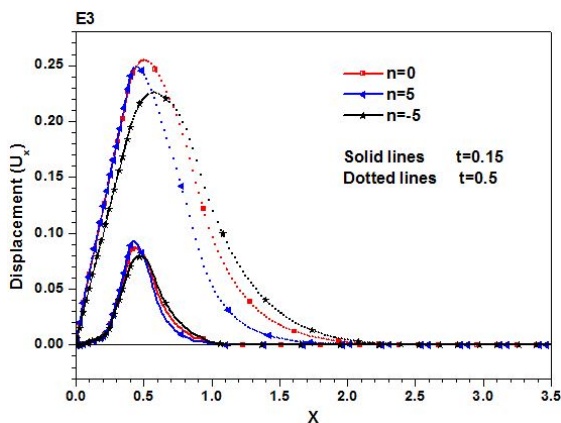


Fig. 13 Displacement U_x distribution along edge OB under different functionally graded parameters at time instants $t = 0.15$ and 0.5

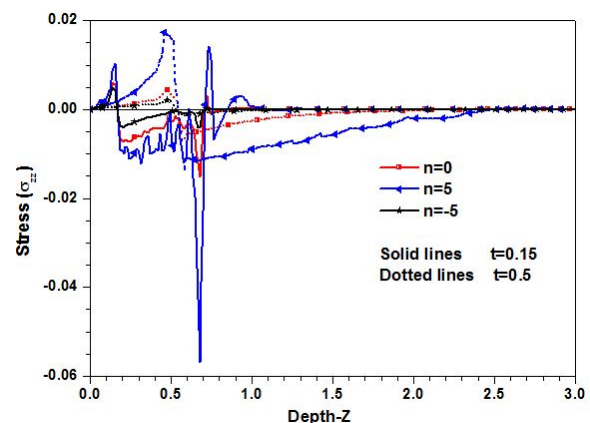


Fig. 14 Stress σ_{zz} distribution along edge OD under different functionally graded parameters at time instants $t = 0.15$ and 0.5

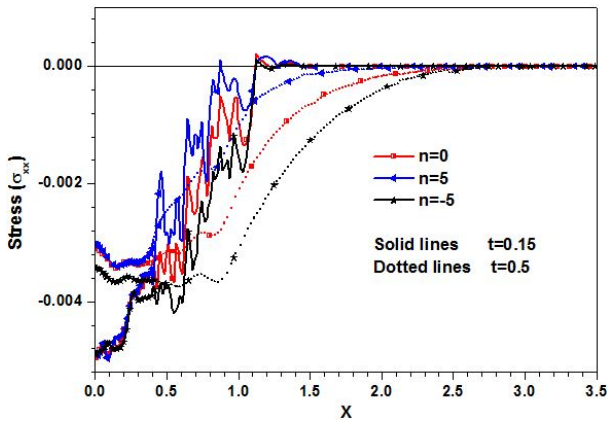


Fig. 15 Stress σ_{zz} distribution along edge OB under different functionally graded parameters at time instants $t = 0.15$ and 0.5

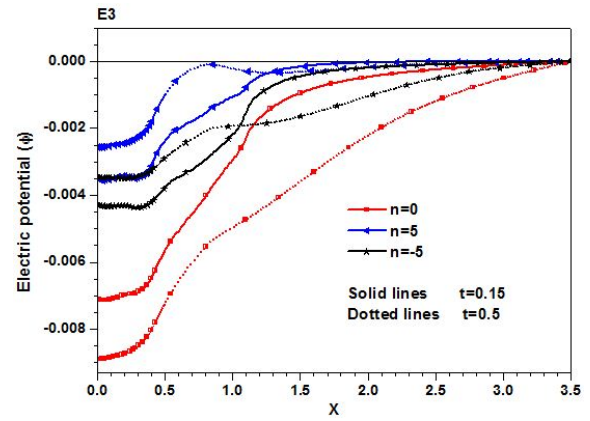


Fig. 17 Electric potential ϕ distribution along edge OB under different functionally graded parameters at time instants $t = 0.15$ and 0.5

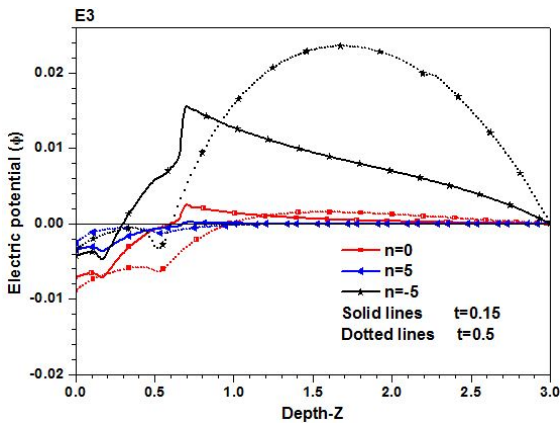


Fig. 16 Electric potential ϕ distribution along edge OD under different functionally graded parameters at time instants $t = 0.15$ and 0.5

stress σ_{zz} is smaller. But for the stress σ_{xx} , the influence of the functionally graded parameter has an opposite trend.

The distributions of electric potential ϕ along edge OD and along edge OB are respectively shown in Figs. 16-17. From Gauss' equation $D_{i,i} = 0$ and the relation between the electric intensity (E) and electric potential $E_i = \phi_{,i}$, the transmission of electric potential is diffused but not in a wave type, i.e., the speed of propagation of electrical potential is infinite. There is not any wave characteristic in the distribution of electric potential, such that there is not a distinct step in the wave front as shown in Figs. 16-17. It can be seen the electric potential on edge OD in material of $n = 5$ is lower than in homogeneous material ($n = 0$) and the electric potential on edge OD in material of $n = -5$ is higher. But for the electric potential on edge OB, the influence of the functionally graded parameter is not obvious. The reason is that the functionally graded parameter is only related with the coordinate z .

Based on the previous analysis and discussion, it can be inferred that the absolute values of responses for the functionally graded material whose parameter is positive (such as $n = 5$) are lower than that of the homogeneous material ($n = 0$) except the stresses and electric potential

along OB. Interestingly, when the functionally graded parameter of material is negative value, the absolute values of responses are the highest compared to the cases of functionally graded parameter greater than zero except the stresses and electric potential along OB. And thus it is possible to make a system of intelligent FGPE materials by combining thermo-piezo-electric materials with functionally graded materials, and the temperature, displacement, stress and electric potential in a FGPE plate can be controlled to implement some functions (such as insulation, the control of the deformation, piezoelectric effect and so on) by regulating the functionally graded parameter of material. In addition, we also find if a thermal or mechanical property of material is functionally graded (such as thermal conductivity, elastic constants), the material can be used to achieve the specific functions (such as controlling the speed of temperature wave and elastic wave), due to space limitations, these results are not shown here.

5. Conclusions

A Finite element governing equations of thermo-piezo-elastic G-L (L-S or C-T) theories are established. Transient thermo-piezo-elastic response of an infinite FGPE plate whose upper surface suffers thermal shock in the context of different thermo-piezo-elastic theories are investigated and analyzed carefully. The problem is solved by using finite element method in time domain directly. We concluded that:

- Temperature distribution predicted by generalized thermo-piezo-elastic theories (G-L and L-S) shows a distinct wave characteristic, i.e., the finite speed of heat propagation. However, the classical thermo-piezo-electric theory (C-T) cannot describe the remarkable characteristic of heat wave.
- Multi-field coupling behaviors between thermal field, deformation and electrical field are presented numerically. Two peaks in stress along Z direction are caused by deformation and thermal wave, respectively. Similarly, two peaks of electrical intensity are induced by combined action of deformation and temperature.

- Functionally graded parameter has a significant influence on transient thermo-piezo-elastic responses of a FGPE plate. It can be expected that transient thermo-piezo-elastic responses, including temperature, displacement, stress and electric potential in a piezoelectric plate are controlled to implement some functions, such as insulation, deformation control and piezoelectric effect by combining thermo-piezo-elastic material with functionally graded material.

Acknowledgments

This study was supported by the National Science Foundation of China (11502085), the Natural Science Foundation of Hubei Province in China (Grant No. 2016CFB542) and the Fundamental Research Funds for the Central Universities (2016YXMS097).

References

- Aouadi, M. (2006), "Generalized thermo-piezoelectric problems with temperature-dependent properties", *Int. J. Solids. Struct.*, **43**(21), 6347-6358.
- Arefi, M. (2015), "The effect of different functionalities of FGM and FGPM layers on free vibration analysis of the FG circular plates integrated with piezoelectric layers", *Smart Struct. Syst., Int. J.*, **15**(5), 1345-1362.
- Arefi, M. and Rahimi, G.H. (2014), "Application of shear deformation theory for two dimensional electro-elastic analysis of a FGP cylinder", *Smart Struct. Syst., Int. J.*, **13**(1), 398-415.
- Babaei, M.H. and Chen, Z.T. (2008), "Dynamic response of a thermopiezoelectric rod due to a moving heat source", *Smart. Mater. Struct.*, **18**(2), 025003.
- Bidgoli, M.R., Karimi, M.S. and Arani, A.G. (2015), "Viscous fluid induced vibration and instability of FG-CNT-reinforced cylindrical shells integrated with piezoelectric layers", *Steel Compos. Struct., Int. J.*, **19**(3), 713-733.
- Chandrasekharaiah, D.S. (1988), "A generalized linear thermo-elasticity theory for piezoelectric media", *Acta. Mech.*, **71**(1-4), 39-49.
- Green, A.E. and Lindsay, K.A. (1972), "Thermoelasticity", *J. Elasticity*, **2**(1), 1-7.
- He, T., Cao, L. and Li, S. (2007), "Dynamic response of a piezoelectric rod with thermal relaxation", *J. Sound. Vib.*, **306**(3), 897-907.
- Heydarpour, Y. and Aghdam, M.M. (2016), "Transient analysis of rotating functionally graded truncated conical shells based on the Lord-Shulman model", *Thin-Wall. Struct.*, **104**, 168-184.
- Khoshgoftar, M.J., Ghorbanpour, A.A. and Arefi, M. (2009), "Thermoelastic analysis of a thick walled cylinder made of functionally graded piezoelectric material", *Smart Struct. Syst.*, **18**(11), 115007.
- Lin, S., Xu, J. and Cao, H. (2016), "Analysis on the Ring-Type Piezoelectric Ceramic Transformer in Radial Vibration", *IEEE. T. Power. Electr.*, **31**(7), 5079-5088.
- Lord, H.W. and Shulman, Y. (1967), "A generalized dynamical theory of thermoelasticity", *J. Mech. Phys. Solids.*, **15**(5), 299-309.
- Ma, Y. and He, T. (2016), "Dynamic response of a generalized piezoelectric-thermoelastic problem under fractional order theory of thermoelasticity", *Mech. Adv. Mater. Struct.*, **23**(10), 1173-1180.
- Mallik, S.H. and Kanoria, M. (2007), "Generalized thermoelastic functionally graded solid with a periodically varying heat source", *Int. J. Solids. Struct.*, **44**(22), 7633-7645.
- Mindlin, R.D. (1961), "On the equations of motion of piezoelectric crystals", *Problems Continuum Mech.*, 282-290.
- Mindlin, R.D. (1974), "Equations of high frequency vibrations of thermopiezoelectric crystal plates", *Int. J. Solids. Struct.*, **10**(6), 625-637.
- Mohammadimehr, M., Rostami, R. and Arefi, M. (2016), "Electro-elastic analysis of a sandwich thick plate considering FG core and composite piezoelectric layers on Pasternak foundation using TSDT", *Steel. Compos. Struct., Int. J.*, **20**(3), 513-543.
- Murali, P. (2008), "Recent progress in materials issues for piezoelectric MEMS", *J. Am. Ceram. Soc.*, **91**(5), 1385-1396.
- Schwab, C. (1998), *p- and hp-finite element methods: Theory and applications in solid and fluid mechanics*. Oxford University Press, Oxford, United Kingdom.
- Shen, Y. and Tian, X. (2014), "Piezothermoelasticity with Finite Wave Speeds", In: *Encyclopedia of Thermal Stresses*, Springer Netherlands, New Delhi, India, pp. 3873-3883.
- Starr, M.B. and Wang, X. (2015), "Coupling of piezoelectric effect with electrochemical processes", *Nano Energy*, **14**, 296-311.
- Tian, X. and Shen, Y. (2005), "Study on generalized magneto-thermoelastic problems by FEM in time domain", *Acta. Mech. Sinica.*, **21**(4), 380-387.
- Tian, X., Shen, Y., Chen, C. and He, T. (2006), "A direct finite element method study of generalized thermoelastic problems", *Int. J. Solids. Struct.*, **43**(7), 2050-2063.
- Tian, X., Zhang, J., Shen, Y. and Lu, T.J. (2007), "Finite element method for generalized piezothermoelastic problems", *Int. J. Solids Struct.*, **44**(18), 6330-6339.
- Tianhu, H., Xiaogeng, T. and Yapeng, S. (2002), "Two-dimensional generalized thermal shock problem of a thick piezoelectric plate of infinite extent", *Int. J. Eng. Sci.*, **40**(20), 2249-2264.
- Tianhu, H., Xiaogeng, T. and Yapeng, S. (2003), "One-dimensional generalized thermal shock problem for a semi-infinite piezoelectric rod", *Acta. Mech. Sinica.*, **35**(2), 158-165.
- Vedavaz, A., Kumar, S. and Moallemi, M.K. (1994), "Significance of non-Fourier heat waves in conduction", *J. Heat. Trans.-T. ASME*, **116**(1), 221-224.
- Xiong, Q.L. and Tian, X.G. (2012), "Thermoelastic study of an infinite functionally graded body with a cylindrical cavity using the Green-Naghdi model", *J. Therm. Stresses.*, **35**(8), 718-732

CC

Nomenclature

T, T_0	Absolute and reference temperature
θ	$= (T - T_0)/T_0$
c_{ijkl}	Elastic constants
e_{ijk}	Piezoelectric coefficients
a_{ij}	Thermal modulus
p_{ij}	Dielectric constants
d_i	Pyroelectric constants
k_{ij}	Thermal conductivity
c_E	Specific heat at constant strain
E_i	Components of electric intensity
ε_{ij}	Components of strain tensor
σ_{ij}	Components of stress tensors
η	entropy density
ρ	Density
ϕ	Electric potential
u, w	Components of displacement vector
q_i	Heat flux
τ, τ_1, τ_2	Thermal relaxation times
D_i	Electric displacement

Subscripts and superscripts

$i(j,k)$	Cartesian coordinate subscript
----------	--------------------------------